# Automated Acquisition of Ground Control Using SAR Layover and Shadows

M. Gelautz [1], E. Mitteregger [1], and F. Leberl [2]

[1] Institute for Computer Vision and Graphics, Technical University Graz,
Münzgrabenstraße 11, A-8010 Graz, Austria
Tel.: ++43/316/873-5031, Fax: ++43/316/873-5050, Email: gelautz@icg.tu-graz.ac.at
[2] Currently on leave and with the Austrian Research Center Seibersdorf,
A-2444 Seibersdorf, Austria

**Abstract** – We present an algorithm which uses SAR layover and shadows for the automated acquisition of ground control. The control points are then utilized to refine the SAR sensor parameters. Tests are carried out on ERS-1 and X-SAR images of the Austrian Alps. The accuracy of the layover/shadow matching algorithm is assessed by comparison with the results obtained by conventional cross-correlation of real-simulated gray value images.

## 1. INTRODUCTION

The acquisition of ground control points (GCPs) between a map and SAR image is an important prerequisite for the geocoding of SAR images, since sensor flight path and other SAR processing parameters are normally only approximately known. However, the manual determination of GCPs constitutes a tedious and time-consuming task, especially in mountainous regions, where terrain induced distortions are strongest. In order to overcome the dissimilarities between the map and image geometry, the use of simulation and subsequent determination of match points between the real and simulated image has been suggested by several authors (e.g., [3], [6], [5], and [2]).

The algorithm we propose is specially suited to SAR imagery of high-relief terrain where layover and shadows occur frequently and are distributed all across the image. It differs from most other simulation based approaches in that it does not require the simulation of the complete gray value image, but only the determination of the location of layover and/or shadows. Thus the problems which are normally associated with the proper modeling of SAR backscatter and the suppression of real-simulated radiometric differences in the matching procedure (see [2]) are avoided.

Previous research on the use of layover and shadows as features for matching was carried out by [7] and [8]. Contrary to our study, the aim of [8] was not to develop a fully automated system, but to provide support to a human operator in an interactive procedure. The algorithm developed by [7] relies on vectorizing shadow boundaries and searching them for points of high curvature. Examples of established correspondences are shown, but no quantitative analysis of the matching accuracy is presented. Layover was not considered in that work.

In the following, we review the principles of our layover/shadow (L/S) matching algorithm and present some results obtained from tests on ERS-1 and X-SAR images of a rugged terrain in the Austrian Alps.

## 2. TEST SITE

Our study area is the Oetztal, a high alpine X-SAR/SIR-C "super-test-site". The area exhibits strong topographic relief, with elevations ranging from 1750 m to more than 3750 m. The available DEM has a grid width of 25 m, and a height accuracy of better than 20 m. It covers an area of approximately 26 km x 16 km.

The layover version of our algorithm was tested on an ERS-1 subscene (23 deg look angle, descending orbit). The matching of shadow features is demonstrated in its application to an X-SAR image acquired during an ascending orbit, at a look angle of 50 deg. Both images have a pixel size of 12.5 m x 12.5 m.

## 3. ALGORITHM

A software has been implemented which first searches a simulated layover and shadow map for suitable features for matching (chips). The presumed L/S regions in the corresponding real image are extracted by thresholding, with the threshold value being derived from the percentage of L/S pixels in the simulated map. A binary overlap technique is applied to compute for each selected chip the location of maximum overlap in the binarized real image. The match points are then employed to refine the SAR imaging model. We perform the parameter refinement by using an already existing optimization modul which is part of the RSG software package [4].

After sensor parameter refinement, the simulation is carried out once more with the now improved imaging model, and the algorithm is applied again to collect a new set of real-simulated match points. This second iteration step allows to verify the success of the previous refinement procedure. If necessary, a further stepwise refinement of the imaging model may be achieved iteratively, with each iteration loop containing the three steps *matching*, *refinement*, and *simulation*, until some predefined accuracy requirement is fulfilled.

## 4. EXPERIMENTS AND RESULTS

We tested our matching algorithm in its application to ERS-1 layover and X-SAR shadows. For both test scenes, the initial simulation parameters were those extracted from the SAR leader files; no previous manual adjustment of the sensor parameters was carried out.

Figs.1 and 2 show the real ERS-1 image before and after thresholding, respectively. The corresponding simulated gray value image is given in Fig.3. The synthetic ERS-1 and X-SAR images are used later to derive correlation based reference matches, in order to compare the results obtained by two different algorithms. The ERS-1 layover map produced by simulation can be seen from Fig.4: Layover areas are displayed in white, and the location of several automatically selected matching chips is marked. In our tests, a smaller chip extension in the range than in azimuth direction appeared to be more suitable than a square template, since it reflects the typical elongated shape of layover. Furthermore, in the spaceborne test data we have investigated until now, the scaling error due to imprecise sensor parameters was found to be clearly bigger in the range than in azimuth direction. Since the binary overlap - like any correlation technique - is based on the assumption of only negligible scaling errors, a too large chip extension in the range direction might therefore produce less accurate correlation results.

A detailed view of the overlap result obtained from one of these chips is presented in Fig.5. Note that there is a well-pronounced peak in the correlation surface shown in (d), which indicates the validity of the match.

A set of 27 (ERS-1) and 25 (X-SAR) match points, distributed all across the area covered by the DEM, was input to the RSG refinement modul. For both images, the main deviation between the assumed and actual image geometry was found to be a shift in both range and azimuth direction. Furthermore, a range scaling error of about 0.3 % was detected for ERS-1.

The simulations were then run again with the refined imaging model and a new set of match points was collected, in order to determine the remaining geometric distortions. Table 1 gives the differences between the absolute location of the real and simulated L/S match points in range ($r$) and azimuth ($a$) direction in terms of the mean value and standard deviation $\sigma$. For comparison, the correlation based matching algorithm CORR developed by [1] was applied to the corresponding real-simulated pairs of gray value images. A mean value and rms error of better than 0.5 pixels and 1.5 pixels, respectively, computed from the new L/S match points demonstrate that the refinement procedure has successfully eliminated the detected distortions. For ERS-1, comparable figures were obtained by algorithm CORR, which confirms our results. The X-SAR results produced by the two algorithms differ slightly more: A difference in $\overline{r}$ of 2.5 pixels, with no notable increase in the corresponding rms values, indicates a systematic shift between the two sets of match points.

Further tests based on threshold variations were carried out to investigate this effect. Generally, the shadow match points were found to be more sensitive to threshold deviations than their layover counterparts. This lack of robustness, together with a slightly asymetric distribution of shadow gray values - in our example, shadow pixels at the near range tended to be darker than at the far range - may be a possible explaination for the observed offset.

*Table 1 Matching results after parameter refinement.*

| Data | Algorithm | $\overline{r}$ pixel | $\sigma_r$ pixel | $\overline{a}$ pixel | $\sigma_a$ pixel |
|---|---|---|---|---|---|
| ERS-1 | L/S (layover) | 0.2 | 1.3 | 0.0 | 1.0 |
| ERS-1 | CORR | 0.2 | 2.2 | 0.9 | 1.3 |
| X-SAR | L/S (shadows) | 0.0 | 1.2 | 0.4 | 1.3 |
| X-SAR | CORR | -2.5 | 1.6 | -0.6 | 1.4 |

## 5. SUMMARY AND DISCUSSION

We have demonstrated that SAR layover and shadows, in conjunction with a binary overlapping technique, can be employed successfully for the automated acquisition of ground control and the subsequent imaging model refinement. After parameter refinement, deviations between the real and simulated ERS-1 image geometry could be described by a mean and rms error of less than 12 m and 28 m, respectively. This result was confirmed by comparison with match points delivered by conventional cross-correlation of image gray values.

The matching algorithm is straightforward, and hence easy to implement and fast. Furthermore, it has proven to be robust to SAR speckle; no previous filtering of the images was required. Regarding robustness to scaling errors, tests on resized images have shown that even at a range scaling error of 25 % corresponding features could still be identified. Further research would be needed to study the influence of inaccurate or low-resolution DEMs on the performance of the matching algorithm. The effects introduced by deviations between the actual and assumed initial sensor parameters are expected to be less critical due to the robustness of the algorithm and the possibility of a successive refinement in several iteration steps.

## 6. ACKNOWLEDGMENTS

The authors wish to thank Scott Hensley from NASA/JPL for providing his matching software. The ERS-1 and X-SAR data were made available by Dr. H. Rott from the University of Innsbruck. We gratefully acknowledge his cooperation. This study was funded by the Austrian Academy of Sciences and the Austrian Ministry of Science.

### 7. REFERENCES

[1] R. Frankot, S. Hensley, and S. Shafer. Noise resistant estimation techniques for SAR image registration and stereo matching. In *Proc. IGARSS'94, Pasadena, CA*, pages 1151–1153, 1994.

[2] B. Guindon. Performance evaluation of real-simulated image matching techniques in the acquisition of ground control for ERS-1 image geocoding. *ISPRS Journal of Photogrammetry and Remote Sensing*, 50(1):2–11, 1995.

[3] B. Guindon and H. Maruyama. Automated matching of real and simulated SAR imagery as a tool for ground control point acquisition. *Can. J. Remote Sensing*, 12(2):149–158, 1986.

[4] Institute for Digital Image Processing, JOANNEUM RESEARCH, Graz. *Remote Sensing Software Package Graz, Software User Manual*, 3.0 edition, 1993.

[5] H. Kimura and T. Iijima. Automated matching of real and simulated SAR imagery for geometric correction. In *Proc. IGARSS'90*, pages 309–312, 1990.

[6] R. Kwok, J. Curlander, and S. Pang. An automated system for mosaicking spaceborne SAR imagery. *Int. J. Remote Sensing*, 11(2):202–223, 1990.

[7] F. Leberl. *Radargrammetric image processing*, chapter 10. Artech House, Norwood, MA, 1990.

[8] M. Plößnig, W. Kropatsch, and D. Strobl. Sherlock supports the geocoding of SAR images. In A. Pinz, editor, *Wissensbasierte Mustererkennung*, pages 112–119. Oldenburg, Vienna, 1989.

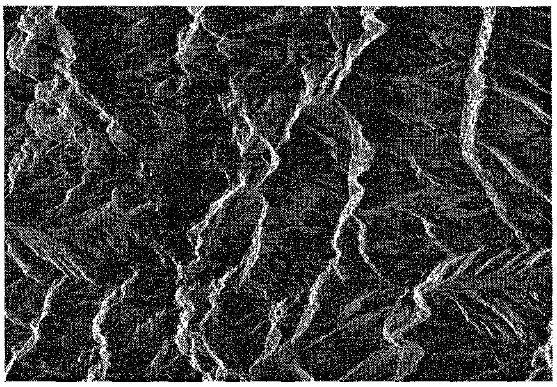

Fig.1 A 2412 x 1679 pixels subsection of an ERS–1 scene acquired of the Oetztal, Austria. The image was illuminated from the right.

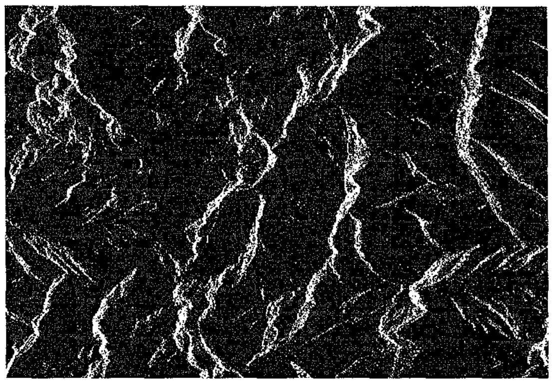

Fig.2 Layover candidates extracted from Fig.1 by thresholding.

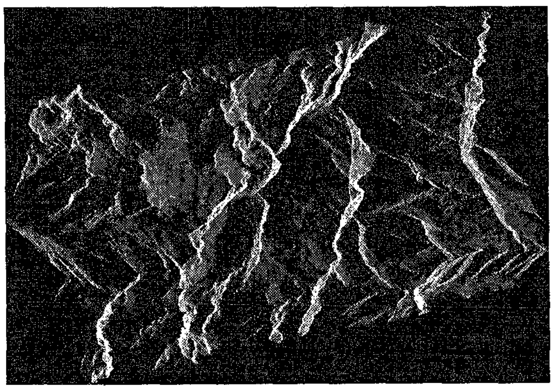

Fig.3 Simulated ERS–1 image corresponding to the actual image from Fig.1. The simulation was produced by assuming a cosine reflectance model.

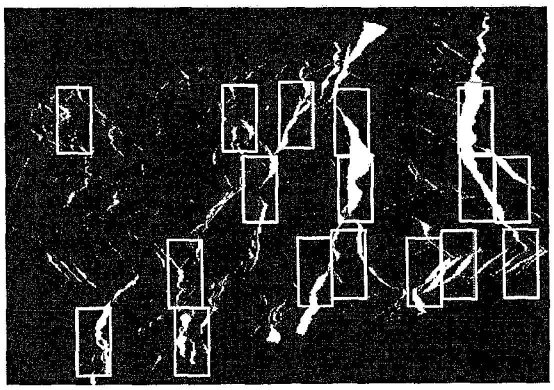

Fig.4 The simulated layover map with examples of automatically selected matching templates. Chip size is 150 x 300 pixels.

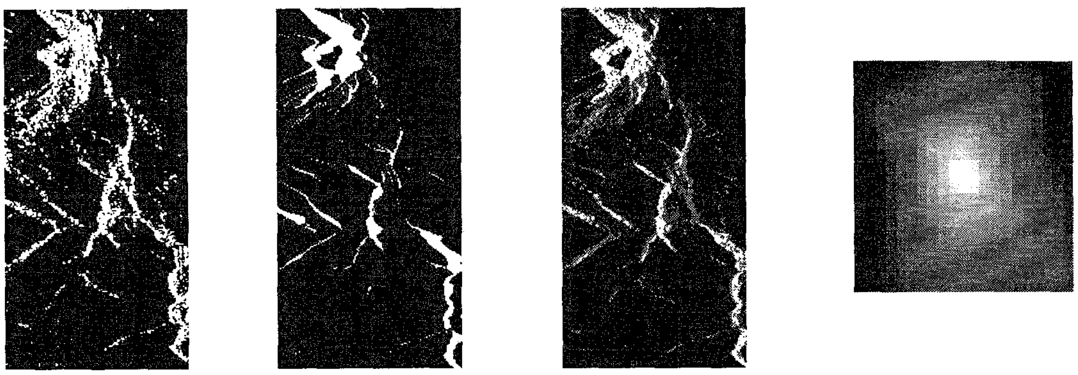

(a) (b) (c) (d)

Fig.5 A detailed view of a real (a) and corresponding simulated (b) chip at the position of maximum overlap (c). White pixels in (c) denote layover in both the real and simulated mask, gray pixels in only one of them. Subfigure (d) shows the gray value encoded correlation surface (21 x 21 pixels).